

Marchaetoglobins A–D: Four Cytochalasans with Proangiogenic Activity from the Marine-Sponge-Associated Fungus *Chaetomium globosum* 162105

Xianxian Miao, Lili Hong, Zhiran Ju, Hongyan Liu, Ruyi Shang, Peihai Li, Kechun Liu, Bin Cheng, Weihua Jiao,* Shihai Xu,* and Houwen Lin*



Cite This: *ACS Omega* 2024, 9, 22450–22458



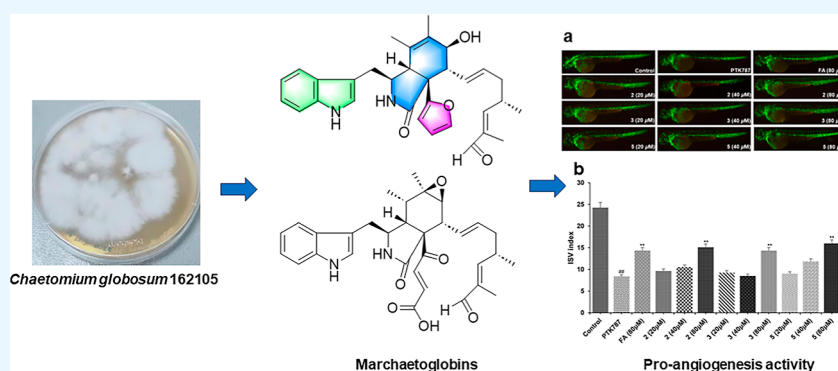
Read Online

ACCESS |

Metrics & More

Article Recommendations

Supporting Information



ABSTRACT: Four new cytochalasans, marchaetoglobins A–D (1–4), along with five known compounds (5–9), were isolated from the marine-sponge-associated fungus *Chaetomium globosum* 162105. Compounds 1–4 represent examples of 19,20-*seco*-chaetoglobosins, of which compound 1 is the first furan-containing cytochalasan. Their structures and absolute configurations were elucidated by extensive spectroscopic analyses and electronic circular dichroism calculations. Compounds 5, 8, and 9 displayed weak to moderate antibacterial activities against *Bacillus thuringiensis*, *Edwardsiella piscicida*, *Vibrio alginolyticus*, and *Pseudomonas syringae* pv. *actinidiae* with minimum inhibitory concentration values ranging from 5 to 25 $\mu\text{g}/\text{mL}$. In addition, compounds 2, 3, and 5 showed potent *in vivo* proangiogenic activity in transgenic zebrafish, comparable to the positive control.

INTRODUCTION

Cytochalasans, a well-established group of fungal metabolites, are characterized by a perhydroisoindolone fused with an 11- to 16-membered macrocyclic ring through the PKS-NRPS hybrid biosynthesis pathway.^{1–3} Based on the amino acids involved in the biosynthesis, cytochalasans could be categorized into six groups of cytochalasins, chaetoglobosins, pyrrihalasins, aspochalasins,alachalasin, and trichalasin.⁴ To date, more than 500 cytochalasans were isolated from fungi, most of which possess a macrocycle bearing either a carbon ring, a lactone, or a cyclic carbonate traditionally.^{5,6} Several cytochalasans with a macrocyclic ring opening, named *seco*-cytochalasans, were reported so far and enriched the structural diversity of the cytochalasan family.⁷ Although these *seco*-cytochalasans account for an extremely small proportion of cytochalasans, they display a wide range of biological activities, notably 19,20-*seco*-cytochalasins. Only 11 19,20-*seco*-cytochalasins named armochaetoglobins A–E,⁸ salchaetoglobosins A and B,⁹ armochaetoglasins B and C,¹⁰ armochaetoglasin L,¹¹ and yamchaetoglobosin A¹² have been reported and display various biological activities including cytotoxic, anti-inflamma-

tory, antitumor, and antimicrobial properties. These 19,20-*seco*-cytochalasans generally exhibited a fatty acid chain attached to C-9, with only armochaetoglobin A displaying a pyrrole functional group. Owing to these intricate and highly functionalized structures, cytochalasans have garnered considerable interest from the chemical and pharmacological scientific communities.⁴

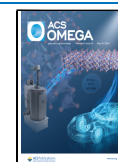
In the search for new cytochalasans from marine fungi, four novel 19,20-*seco*-chaetoglobosins, marchaetoglobins A–D (1–4), together with five known compounds (5–9) (Figure 1) were obtained from the EtOAc extract of *Chaetomium globosum* 162105. To the best of our knowledge, compound 1 is the first isolated cytochalasan containing a furan ring. In

Received: March 14, 2024

Revised: April 12, 2024

Accepted: April 22, 2024

Published: May 8, 2024



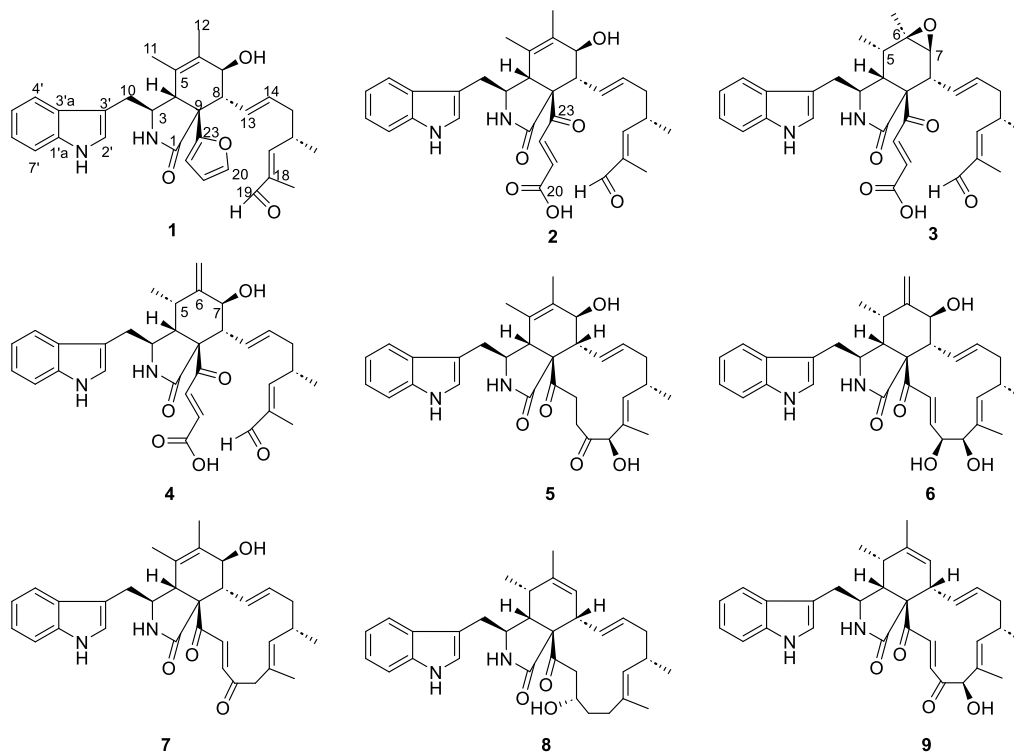


Figure 1. Structures of compounds 1–9.

this study, we present the isolation and structural elucidation as well as antimicrobial and proangiogenic activities of compounds 1–9.

RESULTS AND DISCUSSION

The molecular formula $C_{32}H_{36}N_2O_4$ of marchaeotoglobin A (**1**), with 16 double-bond equivalents, was deduced from the protonated ion peak at m/z 513.2754 $[M + H]^+$ in the HRESIMS spectrum. The IR spectrum exhibited strong absorbance bands for the hydroxy (3336 cm^{-1}) and carbonyl (1677 cm^{-1}) groups. The ^1H NMR spectrum of **1** (Table 1) displayed five aromatic protons assignable to a 3-substituted indolyl moiety [δ_{H} 7.07 (1H, t, $J = 7.2\text{ Hz}$), 7.32 (1H, q, $J = 7.8\text{ Hz}$), 6.97 (1H, t, $J = 7.4\text{ Hz}$), 6.84 (1H, s), and 7.30 (1H, q, $J = 8.1\text{ Hz}$)]. Six aromatic or olefinic protons [δ_{H} 7.54 (1H, s), 6.36 (1H, s), 6.19 (1H, d, $J = 2.6\text{ Hz}$), 6.03 (1H, dd, $J = 15.3, 9.6\text{ Hz}$), 5.10 (1H, m), and 6.30 (1H, d, $J = 9.8\text{ Hz}$)] and one aldehyde proton [δ_{H} 9.30 (1H, s)] were also observed. Detailed analysis of the ^{13}C NMR and HSQC spectra revealed the presence of 32 carbon resonances, including four methyls, two methylenes, 17 methines (one aldehyde at δ_{C} 197.6, 11 olefinic or aromatic at δ_{C} 108.4, 111.3, 131.8, 131.8, 142.7, 162.2, 112.3, 119.1, 119.7, 122.4, and 124.5), and nine nonprotonated carbons (one carbonyl at δ_{C} 177.5, four olefinic or aromatic at δ_{C} 128.0, 133.9, 138.9, and 156.9).

The planar structure was elucidated by ^1H – ^1H COSY and HMBC spectra (Figure 2). The HMBC correlations from H-4' to C-1'a and C-3'a, from H-2' to C-1'a, C-3'a, and C-3', and from H-7' to C-1'a, combined with COSY correlations of H-4'/H-5'/H-6'/H-7', allowed for the construction of a 3-substituted indolyl moiety. Meanwhile, the core structure isoindolone moiety was established by consecutive ^1H – ^1H COSY correlations of H-3/H-4 and H-7/H-8, coupled with the long-range HMBC correlations from H-4 to C-1 and C-5, from H₃-11 to C-4, C-5, and C-6, from H₃-12 to C-5, C-6, and

C-7, and from H-8 to C-9 and C-1. The location of the 3-substituted indolyl moiety was assigned to C-3 through C-10 by the HMBC correlations from H-10 to C-2', C-3', and C-3'a and COSY correlations from H-3 to H-10. The aliphatic chain at C-8 was deduced from the HMBC correlations from 16-Me to C-15, C-16, and C-17 and from 18-Me to C-17, C-18, and C-19, coupled with COSY cross-peaks of H-8/H-13/H-14/H-15/H-16/H-17. The HMBC correlations from H-20 and H-22 to C-23 and the ^1H – ^1H COSY correlations of H-20/H-21/H-22 demonstrated the presence of the furan ring. In addition, the HMBC correlations from H-8 to C-23 indicated that the furan ring was attached at C-9. Finally, the rest of the OH in the molecular formula and its location at C-7 (δ_{H} 3.92, δ_{C} 71.0) were assigned in **1**. The planar structure of **1** was thus elucidated as shown in Figure 2.

The structure of **1** totally possesses 6 stereocenters, and the relative configuration of **1** was evidenced by J -based configuration analysis and the ROESY experiment (Figure 3). The large coupling constant of $J_{1,14}$ (15.3 Hz) and the ROESY correlation of H-16/18-Me suggested the *E*-geometry of $\Delta^{13,14}$ and $\Delta^{17,18}$. The ROESY correlations of H₃-11/H₃-3, H₃-11/H₃-12, H₃-12/H-7, and H-7/H-13 indicated that they were cofacial, assigned as being in the α -orientation. Moreover, the ROESY interactions of H-4 with H-8, H-10, and H-22 revealed the β -orientation of H-4 and H-8 and the *cis* ring junction of the pyrrolidine-2-one moiety and cyclohexane ring.

The absolute configuration of compound **1** was determined by comparison of the calculated electronic circular dichroism (ECD) using TDDFT performed with Gaussian 09 program. The ECD spectra of 3*S*,4*R*,7*S*,8*R*,9*R*,16*R*-**1** and 3*S*,4*R*,7*S*,8*R*,9*R*,16*S*-**1** were measured by Boltzmann distribution theory and relative Gibbs free energy (ΔG). The experimental ECD curves displayed a good agreement with the calculated ECD spectra of 3*S*,4*R*,7*S*,8*R*,9*R*,16*R*-**1** and 3*S*,4*R*,7*S*,8*R*,9*R*,16*S*-**1** (Figure 4). Thus, the absolute config-

Table 1. ^1H and ^{13}C NMR Spectroscopic Data for Compounds **1** and **2**^a

no.	1		2	
	δ_{H}	δ_{C}	δ_{H}	δ_{C}
1		177.5, C		176.0, C
3	3.55 (dd, 9.6, 6.0)	60.1, CH	3.58 (m)	59.5, CH
4	3.09 (s)	51.9, CH	3.16 (s)	48.4, CH
5		128.0, C		133.6, C
6		133.9, C		128.0, C
7	3.92 (d, 7.8)	71.0, CH	3.85 (d, 7.8)	71.1, CH
8	2.51 (m)	53.1, CH	2.72 (m)	51.1, CH
9		52.5, C		63.9, C
10	2.77 (dd, 14.0, 5.4)	32.5, CH ₂	2.88 (m)	33.3, CH ₂
	2.50 (m)		2.74 (m)	
11	1.17 (s)	17.3, CH ₃	1.34 (s)	17.6, CH ₃
12	1.64 (s)	14.8, CH ₃	1.67 (s)	15.6, CH ₃
13	6.03 (dd, 15.3, 9.6)	131.8, CH	5.96 (dd, 15.1, 9.1)	130.4, CH
14	5.10 (m)	131.8, CH	5.43 (m)	133.7, CH
15	2.03 (m)	40.3, CH ₂	2.11 (m)	40.3, CH ₂
16	2.62 (m)	35.0, CH	2.73 (m)	34.8, CH
17	6.30 (d, 9.8)	162.2, CH	6.35 (d, 9.8)	161.8, CH
18		138.9, C		139.2, C
19	9.30 (s)	197.6, CH	9.31 (s)	197.7, CH
20	7.54 (s)	142.7, CH		173.3, C
21	6.36 (s)	111.3, CH	6.85 (d, 15.4)	140.9, CH
22	6.19 (d, 2.6)	108.4, CH	7.40 (d, 15.2)	132.3, CH
23		156.9, C		200.1, C
2'	6.84 (s)	124.5, CH	7.00 (m)	124.6, CH
3'		111.8, C		111.4, C
3'a		128.6, C		128.5, C
4'	7.30 (q, 8.1)	119.1, CH	7.50 (d, 7.8)	119.2, CH
5'	6.97 (t, 7.4)	119.7, CH	7.04 (m)	119.9, CH
6'	7.07 (t, 7.2)	122.4, CH	7.08 (t, 15.0)	122.5, CH
7'	7.32 (q, 7.8)	112.3, CH	7.34 (d, 8.1)	112.4, CH
1'a		138.1, C		138.2, C
16-CH ₃	0.96 (d, 6.7)	19.5, CH ₃	1.04 (d, 6.7)	19.5, CH ₃
18-CH ₃	1.68 (s)	9.3, CH ₃	1.69 (s)	9.3, CH ₃

^aRecorded at 600 MHz (^1H) and 150 MHz (^{13}C) in methanol-*d*₄.

uration of **1** was assigned as 3*S*,4*R*,7*S*,8*R*,9*R*, with C-16 being unsolved. Taking the biosynthetic pathway of cytochalasans into consideration,^{13,14} the configuration of C-16 was determined as *S*. These data confirmed compound **1**, as a new 19,20-*seco*-chaetoglobosin alkaloid, which is characterized by a bicyclic isoindolone integrated with an aliphatic chain, a furan ring, and an indolyl group. To the best of our knowledge, this is the first isolation of cytochalasan with a furan ring.

The molecular formula of marchaeoglobin B (**2**) was determined as C₃₂H₃₆N₂O₆ by HRESIMS and NMR data, which corresponded to 16 degrees of unsaturation. The 1D NMR data of **2** (Table 1) exhibited close similarity to those of **1** except for an aliphatic chain (C-20–C-23) instead of a furan ring at C-9 in **1**. This assumption was corroborated by the HMBC correlations from H-21 to C-20 and C-23, from H-22 to C-23, and from H-4 to C-23, as well as the ^1H – ^1H COSY spin system of H-21/H-22. Detailed ROESY analysis (Figure 3) and biosynthetic considerations suggested that **2** possessed the same relative configurations of **1**.^{13,14} As shown in Figure 4, the experimental ECD curves of **2** matched well with the calculated ECD curves of (3*S*,4*R*,7*S*,8*R*,9*R*)-**2** and assigned the

absolute configuration of **2** as 3*S*,4*R*,7*S*,8*R*,9*R*. The configuration of C-16 was the same as that in compound **1** based on the biosynthetic considerations.

HRESIMS data of marchaeoglobin C (**3**) showed a protonated molecule at *m/z* 545.2646 [*M* + *H*]⁺ (calcd for C₃₂H₃₇N₂O₆, 545.2652), accountable to a molecular formula of C₃₂H₃₆N₂O₆, isomeric to **2**. The NMR data for **3** were nearly akin to those of **2**, with a few notable exceptions. The difference observed in **3** was the occurrence of signals corresponding to an epoxide unit (δ_{C} = 58.8, 62.8; δ_{H} = 2.83) and the hydrogenation of a carbon–carbon double bond (δ_{C} = 58.8, 37.1; δ_{H} = 1.84). This assignment was confirmed by the HMBC correlations from H₃-11 to C-4, C-5, and C-6 and from H₃-12 to C-5, C-6, and C-7. The relative configuration of **3** was deduced by a ROESY experiment. The large coupling constant of *J*_{13,14} (15.1 Hz) and *J*_{21,22} (15.4 Hz) and the ROESY correlation of H-16/18-Me indicated the *E*-geometry of $\Delta^{13,14}$, $\Delta^{21,22}$, and $\Delta^{17,18}$.

The ROESY correlations of H₃-11/H-3, H₃-12/H-3, and H₃-12/H-7 indicated that they were assigned as being in the α -orientation. Furthermore, the ROESY interactions of H-4 with H-10 and H-22 revealed the β -orientation of H-4 and the *cis* ring junction of the pyrrolidine-2-one and the cyclohexane moiety (Figure 3). The absolute configuration of **3** was assigned as 3*S*,4*R*,5*S*,6*R*,7*S*,8*R*,9*R*,16*S* based on ECD calculation (Figure 4) and the biosynthetic pathway of cytochalasans.^{13,14}

The HRESIMS spectrum of marchaeoglobin D (**4**) exhibited a molecular formula of C₃₂H₃₆N₂O₆, isomeric with **2**. The NMR data closely resembled those of **2** except for the double bond $\Delta^{5,6}$ in **2** being transferred to $\Delta^{6,12}$ in **4**. This deviation was established by the NMR signals due to an exocyclic olefin (δ_{C} 113.9; δ_{H} 5.21, 5.03) and HMBC correlations from H₂-12 to C-5 and C-7. The ROESY correlations of H₃-11/H-3, H-3/H-12, and H-12/H-7 indicated that they were cofacial, assigned as being in the α -orientation. Moreover, the ROESY interactions of H-4 with H-8 revealed the β -orientation (Figure 3). The absolute configuration of **4** was assigned as 3*S*,4*R*,5*S*,7*S*,8*R*,9*R*,16*S* by comparison of the experimental and calculated ECD spectra of **4** (Figure 4) and the biosynthetic pathway of cytochalasans.^{13,14}

Five known compounds were identified as chaetoglobosin O (**5**),¹⁶ cytoglobosin B (**6**),¹⁵ prochaetoglobosin IIIed (**7**),¹⁷ armochaetoglasin F (**8**),¹⁰ and chaetoglobosin J (**9**)¹⁸ by interpretation of spectroscopic data and comparison with the reported data.

We next investigated the proangiogenic and antibacterial activities of compounds **1**–**9**. The *in vivo* proangiogenic activity of the isolates was evaluated in transgenic fluorescent zebrafish Tg(vegfr2-GFP) mode. As shown in Figure 5, compounds **1**–**3** and **5**–**7** increased the number of intersegmental blood vessels (ISVs) in zebrafish at a concentration of 40 $\mu\text{g}/\text{mL}$. Next, a transgenic fluorescent zebrafish Tg(flk1:EGFP) model was used to further confirm the proangiogenic activity of compounds **1**–**3**, **5**, and **7** at different concentrations. The quantitative analysis revealed that compounds **2**, **3**, and **5** exhibited potent proangiogenic activities at a concentration of 80 μM , comparable to the positive control (Figure 6). Additionally, the antibacterial activity screening showed that compounds **5**, **8**, and **9** displayed weak to moderate inhibitory effects against *Bacillus thuringiensis*, *Edwardsiella piscicida*, *Vibrio alginolyticus*, and

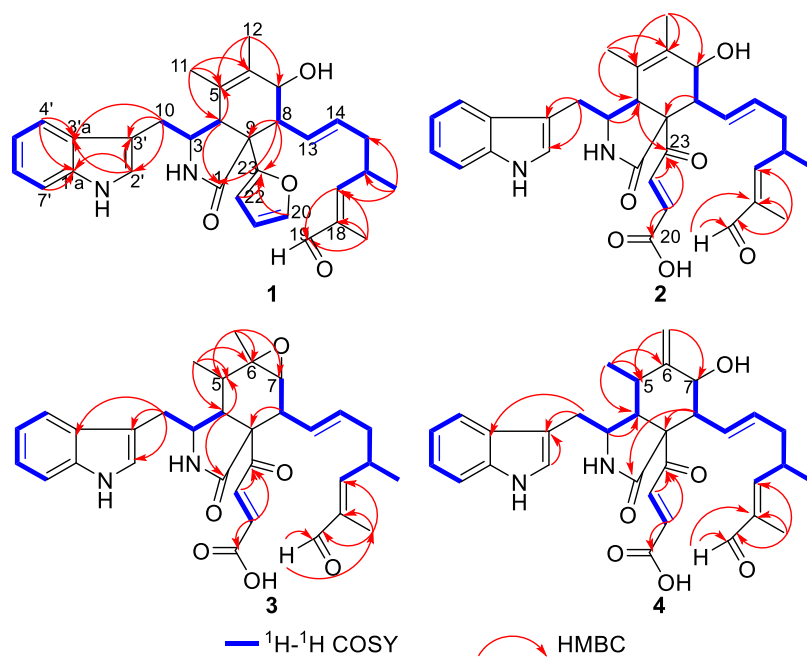


Figure 2. Key 2D NMR correlations of compounds 1–4.

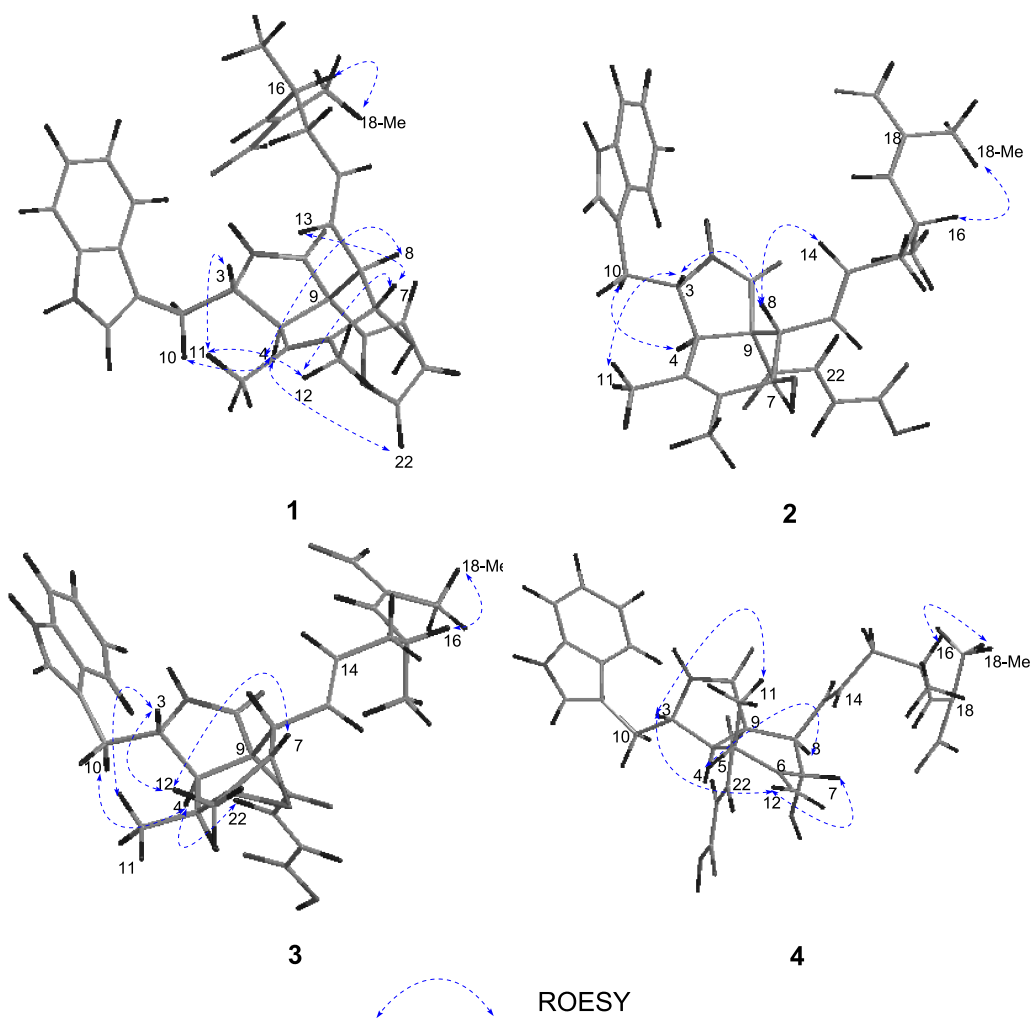


Figure 3. Key ROESY correlations of compounds 1–4.

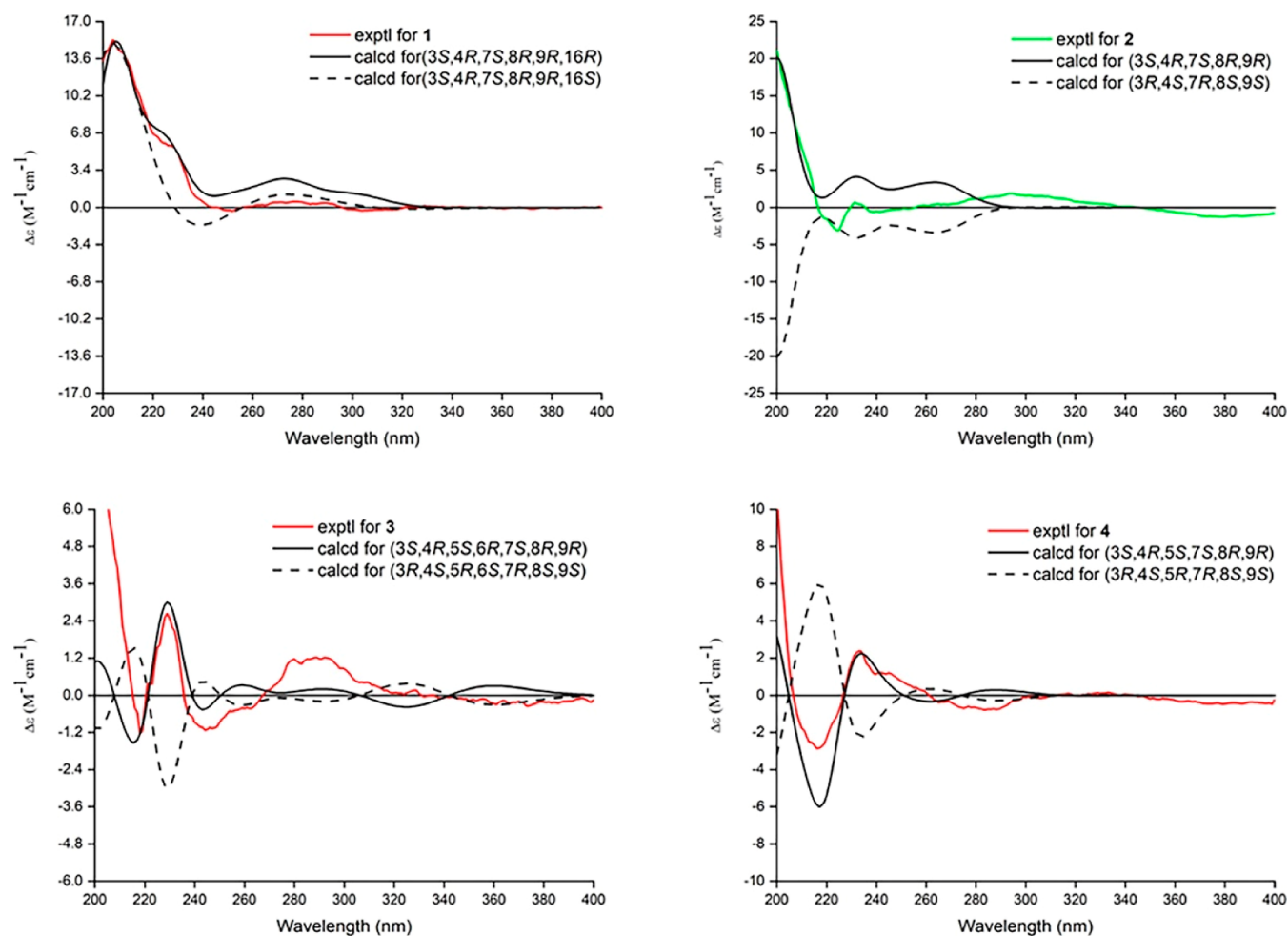


Figure 4. Experimental and calculated ECD spectra of compounds 1–4.

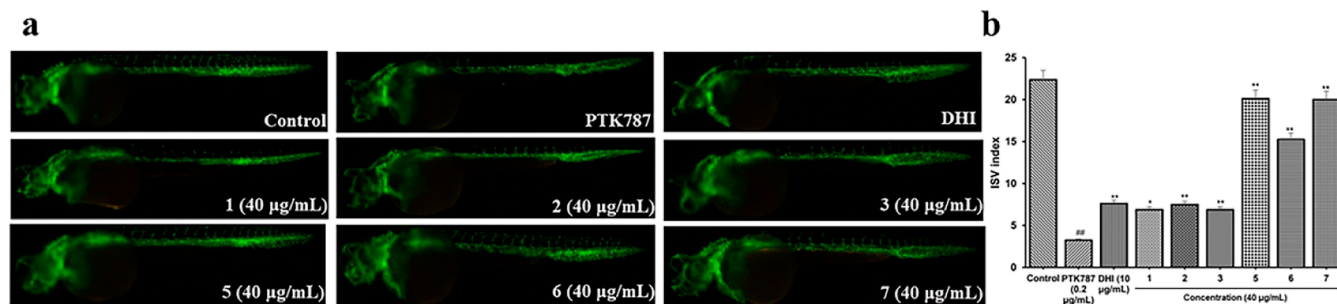


Figure 5. (a) Images of intersomitic vessels (ISVs) in transgenic fluorescent zebrafish Tg(vegfr2:GFP) embryos treated with compounds 1–3 and 5–7 (40 $\mu\text{g}/\text{mL}$), using Danhong injection (DHI) (10 $\mu\text{g}/\text{mL}$) as a positive control. (b) Quantitative analysis of the number of ISVs in transgenic fluorescent zebrafish Tg(vegfr2:GFP) embryos treated with compounds 1–3 and 5–7. Data were represented as mean \pm SD. ## $p < 0.01$ compared to the control group. ** $p < 0.01$ and * $p < 0.05$ compared to the PTK787 model group.

Pseudomonas syringae pv. *actinidiae* with minimum inhibitory concentration (MIC) values ranging from 5.0 to 25 $\mu\text{g}/\text{mL}$ (Table 3).

CONCLUSIONS

In summary, four new cytochalasan alkaloids were isolated and characterized from marine-sponge-derived *C. globosum* 162105. Compounds 1–4 are 19,20-*seco*-chaetoglobosins with only 11 members of this type of cytochalasans. Marchaetoglobin A (1), the first example of cytochalasan bearing a furan ring, is of great importance in enriching the chemistry diversity of

cytochalasan and deserves further exploration of the biosynthetic pathway. Compounds 2, 3, and 5 exhibit appealing proangiogenesis activity, while compound 9 demonstrates antibacterial activity, suggesting that these cytochalasans are worthy of further study as potential new drugs.

EXPERIMENTAL SECTION

General Experimental Procedures. Optical rotation measurements were determined using an Autopol VI, serial no. 91003, manufactured by Rudolph Research Analytical Hackettstown, NJ, USA. IR and UV spectra were obtained on a

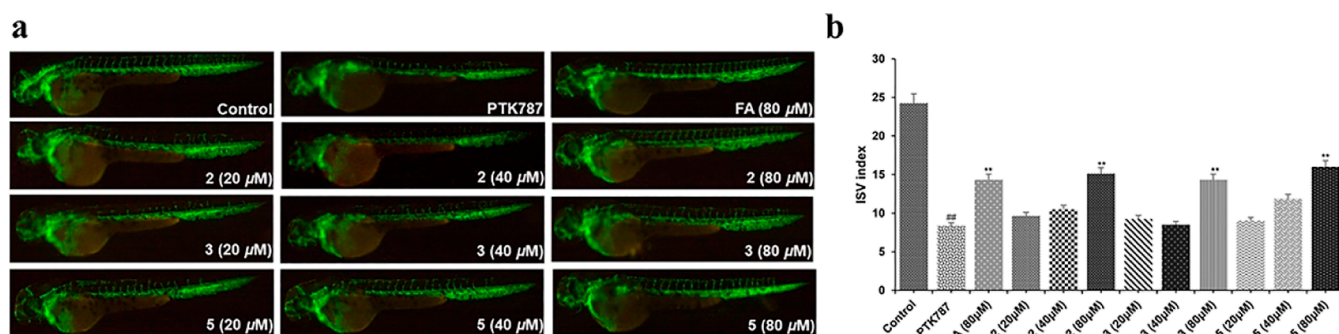


Figure 6. (a) Images of intersomitic vessels (ISVs) in transgenic fluorescent zebrafish Tg(flk1: EGFP) embryos treated with different concentrations (20, 40, and 80 μM) of compounds 2, 3, and 5, using ferulic acid (80 μM) as a positive control. (b) Quantitative analysis of the number of ISVs in transgenic fluorescent zebrafish Tg(flk1:EGFP) embryos treated with compounds 2, 3, and 5. Data were represented as mean \pm SD. $\#p < 0.01$ compared to the control group; $**p < 0.01$ compared to the PTK787 model group.

Table 2. ^1H and ^{13}C NMR Spectroscopic Data for Compounds 3 and 4^a

no.	3		4	
	δ_{H}	δ_{C}	δ_{H}	δ_{C}
1		176.2, C		175.8, C
3	3.79 (t, 6.9)	54.9, CH	3.51 (t, 6.54)	54.2, CH
4	2.65 (m)	48.2, CH	2.66 (q, 7.6)	48.1, CH
5	1.84 (t, 7.08)	37.1, CH	2.88 (m)	32.5, CH
6		58.8, C		151.2, C
7	2.83 (d, 7.8)	62.8, CH	3.97 (d, 9.4)	73.2, CH
8	2.80 (m)	46.4, CH	3.03 (t, 9.5)	49.0, CH
9		65.8, C		64.4, C
10	2.94 (dd, 13.8, 5.1)	34.3, CH ₂	2.90 (m)	33.7, CH ₂
	2.62 (m)		2.74 (m)	
11	0.67 (d, 7.2)	12.9, CH ₃	0.74 (s)	13.6, CH ₃
12	1.17 (s)	19.8, CH ₃	5.21 (s)	113.9, CH ₂
			5.03 (s)	
13	6.11 (dd, 15.1, 9.1)	130.0, CH	5.96 (dd, 15.1, 9.1)	130.4, CH
14	5.54 (m)	133.1, CH	5.51 (m)	133.5, CH
15	2.16 (m)	40.2, CH ₂	2.14 (m)	40.3, CH ₂
16	2.78 (m)	34.7, CH	2.77 (m)	34.7, CH
17	6.36 (d, 9.8)	161.5, CH	6.40 (d, 9.6)	161.8, CH
18		139.4, C		139.2, C
19	9.33 (s)	197.7, CH	9.35 (s)	197.7, CH
20		173.0, C		172.9, C
21	6.81 (d, 15.4)	142.0, CH	6.80 (d, 15.3)	141.5, CH
22	7.11 (d, 15.2)	131.7, CH	7.23 (d, 15.3)	132.0, CH
23		199.7, C		199.3, C
2'	7.00 (s)	124.7, CH	7.02 (m)	124.7, CH
3'		110.9, C		111.0, C
3'a		128.7, C		128.8, C
4'	7.48 (d, 7.8)	119.1, CH	7.49 (d, 7.8)	119.1, CH
5'	7.01 (d, 7.2)	120.0, CH	7.04 (m)	119.6, CH
6'	7.07 (t, 15.0)	122.5, CH	7.10 (t, 15.3)	122.4, CH
7'	7.32 (d, 8.1)	112.4, CH	7.35 (d, 8.2)	112.4, CH
1'a		138.1, C		138.1, C
16-CH ₃	1.03 (d, 6.7)	19.5, CH ₃	1.04 (d, 6.7)	19.4, CH ₃
18-CH ₃	1.70 (s)	9.3, CH ₃	1.72 (s)	9.3, CH ₃

^aRecorded at 600 MHz (^1H) and 150 MHz (^{13}C) in methanol-*d*₄.

Thermo Fisher Nicolet iS50 spectrometer and a Persee TU-1950-YV-VIS spectrophotometer, respectively. ECD spectra were recorded on a Jasco-J-810 spectropolarimeter. NMR

spectroscopic data were acquired on a Bruker AV-600 MHz spectrometer in methanol-*d*₄ (δ_{H} 3.31; δ_{C} 49.0). HRESIMS was obtained in positive ion mode on a Waters Xevo G2-XS/APGC spectrometer. Preparative MPLC was used in a Interchim Puriflash 450 instrument. Column chromatography (CC) was carried out using silica gel (200–300 mesh; Yantai) and ODS C₁₈ (15 μm , Santai Technologies, Inc.). Analytical thin-layer chromatography was performed on a silica gel FSGF₂₅₄ plate. A YMC-Pack Pro C₁₈ column (250 \times 10 mm, 5 μm) was used for reversed-phase HPLC using a Waters 1525 separation module equipped with a Waters 2535 pump and a 2998 photodiode array detector.

Fungus Material. The fungus *C. globosum* 162105 was isolated from the inner tissue of the marine sponge *Dysidea* sp. collected from Yongxing Island in the South China Sea in May 2015 and was deposited at $-80\text{ }^\circ\text{C}$. A voucher specimen was maintained at the Research Center for Marine Drugs, State Key Laboratory of Oncogenes and Related Genes, Department of Pharmacy, Renji Hospital, School of Medicine, Shanghai Jiao Tong University.

Fermentation, Extraction, and Isolation. The fungus *C. globosum* was grown in potato dextrose agar medium in a Petri dish for 7 days. Then its spores were directly inoculated into 250 mL Erlenmeyer flasks each containing 100 mL of the seed medium (potato 200 g/L, dextrose 20 g/L, and artificial seawater salts 30 g/L in purified H₂O) on a rotatory shaker with 180 rpm at 28 $^\circ\text{C}$ for 72 h. The subsequent amplified fermentation was carried out in 30 \times 2 L Erlenmeyer flasks. Each flask contained 80 g of rice, 120 mL of distilled H₂O, and 2 g of artificial seawater salts, where 20 mL of the seed culture was transferred and incubated under static conditions at 25 $^\circ\text{C}$ for 35 days. The fermented substrate was first extracted with MeOH. Then the combined residue was further extracted with EtOAc, yielding 42 g of extract after removal of the organic solvent under reduced pressure.

The crude extract was applied to Sephadex LH-20 eluted with a petroleum ether/dichloromethane/methanol (4:5:1) mixture to give 11 fractions (Frs. E1–E11). Fr. E5 (9.6 g) was subjected to CC on silica gel, eluting with a petroleum ether/ethyl acetate gradient system (from 50:1 to 0:1), to give 12 fractions (Fr. E5A–E5L). Subfraction E5H (2.3 g) was separated by reversed-phase ODS MPLC (5–100% MeCN/H₂O, 540 min, flow rate 20 mL/min, UV detection at 210, 220, and 280 nm) to afford 13 fractions (Frs. E5H1–Fr. E5H13). Fr. E5H5 (30 mg) was then purified by semi-preparative reversed-phase HPLC (XBridge C18, 10 \times 250

Table 3. Antimicrobial Assay of Compounds 1–9 (MIC Values in $\mu\text{g/mL}$)

comp. ^a	antimicrobial assay			
	<i>Bacillus thuringiensis</i>	<i>Pseudomonas syringae</i> pv. <i>actinidiae</i>	<i>Vibrio alginolyticus</i>	<i>Edwardsiella piscicida</i>
5	25			
8		10	25	10
9		5	5	
Chloramphenicol (CPL) ^b	2	2	2	2

^aCompounds 1–4 and 6–7 were inactive (MIC > 50 $\mu\text{g/mL}$) for all tested strains. ^bPositive control substance.

mm, 2 mL/min) eluted with 35% MeCN in H₂O to yield 7 (1.5 mg, t_{R} = 45.0 min) and 8 (2.5 mg, t_{R} = 60.7 min). Subfraction E5L (3.0 g) was separated by reversed-phase ODS MPLC (5–100% MeCN/H₂O, 640 min, flow rate 25 mL/min, UV detection at 210, 220, and 280 nm) to afford 15 fractions (Frs E5L1–Fr E5L15). Compounds 1 (2.2 mg), 5 (3.2 mg), and 9 (4.0 mg) were purified using reversed-phase HPLC (27% MeCN/H₂O, 9 for t_{R} = 30.0 min, 5 for t_{R} = 56.0 min, 1 for t_{R} = 180.0 min) from Fr. E5L10 (150.0 mg). Fr. E5M (1.5 g) was separated by reversed-phase ODS MPLC (5–100% MeCN/H₂O, 600 min, flow rate 20 mL/min, UV detection at 210, 220, and 280 nm) to afford compounds 2 (4.0 mg, t_{R} = 75.0 min) and 3 (3.6 mg, t_{R} = 100.5 min). Compound 4 (1.5 mg, t_{R} = 85.0 min) was separated from Fr. E5N (1.0 g) under the same separation conditions as compounds 2 and 3. Fr. E10 (1.1 g) was separated by reversed-phase ODS MPLC (5–100% MeCN/H₂O, 540 min, flow rate 20 mL/min, UV detection at 210, 220, and 280 nm) to afford 7 fractions (Frs. E10A–E10G). Fr. E10F (75 mg) was then purified by semipreparative reversed-phase HPLC (XBridge C18, 10 × 250 mm, 2 mL/min) eluted with 27% MeCN in H₂O to yield 6 (1.0 mg, t_{R} = 45.0 min).

Marchaetoglobin A (1). Pale yellow, amorphous powder; $[\alpha]_{\text{D}}^{20}$ +20 (MeOH c 0.10); UV (MeOH) λ_{max} (log ϵ): 193 (1.17), 222 (1.38), 282 (0.15) nm; ECD (MeOH) λ_{max} ($\Delta\epsilon$): 204 (+1.39), 229 (+0.49), 278 (+0.048) nm; IR (KBr) ν_{max} : 3336, 2958, 2922, 1877, 1677, 1584, 1412, 1236, 1099, 1022, 875, 822, 739 cm^{-1} ; ¹H NMR (600 MHz, CD₃OD) and ¹³C NMR (150 MHz, CD₃OD) data, see Table 1; HRESIMS data at m/z 513.2754 [M + H]⁺ (calcd for C₃₂H₃₇N₂O₄, 513.2753).

Marchaetoglobin B (2). White powder; $[\alpha]_{\text{D}}^{20}$ +79 (MeOH c 0.46); UV (MeOH) λ_{max} (log ϵ): 194 (2.17), 223 (1.81), 281 (0.26) nm; ECD (MeOH) λ_{max} ($\Delta\epsilon$): 199 (+1.58), 225 (−0.22), 233 (+0.02), 296 (+0.12) nm; IR (KBr) ν_{max} : 3333, 2959, 2851, 1682, 1599, 1452, 1384, 1259, 1100, 978, 802, 743 cm^{-1} ; ¹H NMR (600 MHz, CD₃OD) and ¹³C NMR (150 MHz, CD₃OD) data, see Table 1; HRESIMS data at m/z 545.2653 [M + H]⁺ (calcd for C₃₂H₃₇N₂O₆, 545.2652).

Marchaetoglobin C (3). White amorphous powder; $[\alpha]_{\text{D}}^{20}$ +17 (MeOH c 0.31); UV (MeOH) λ_{max} (log ϵ): 193 (2.00), 224 (1.86), 282 (0.25) nm; ECD (MeOH) λ_{max} ($\Delta\epsilon$): 199 (+0.65), 219 (−0.06), 229 (+0.14), 247 (−0.05), 288 (+0.06) nm; IR (KBr) ν_{max} : 3341, 2920, 2825, 1685, 1604, 1379, 1357, 1258, 1152, 1096, 1027, 974, 880, 803, 742 cm^{-1} ; ¹H NMR (600 MHz, CD₃OD) and ¹³C NMR (150 MHz, CD₃OD) data, see Table 2; HRESIMS data at m/z 545.2646 [M + H]⁺ (calcd for C₃₂H₃₇N₂O₆, 545.2652).

Marchaetoglobin D (4). White amorphous powder; $[\alpha]_{\text{D}}^{20}$ +52 (MeOH c 0.10); UV (MeOH) λ_{max} (log ϵ): 193 (2.03), 222 (1.34), 290 (0.40) nm; ECD (MeOH) λ_{max} ($\Delta\epsilon$): 192 (+3.60), 217 (−0.42), 234 (+0.35), 289 (−0.11) nm; IR (KBr) ν_{max} : 3324, 2959, 2923, 1675, 1597, 1452, 1381, 1258, 1235, 1098, 1030, 977, 870, 798, 742 cm^{-1} ; ¹H NMR (600

MHz, CD₃OD) and ¹³C NMR (150 MHz, CD₃OD) data, see Table 2; HRESIMS data at m/z 545.2647 [M + H]⁺ (calcd for C₃₂H₃₇N₂O₆, 545.2652).

■ BIOLOGICAL ASSAY

Proangiogenic Activity Assay. *Embryo Acquisition of Zebrafish.* Tg(vegfr2:GFP) and Tg(flkl1:EGFP) transgenic zebrafish were provided by the Engineering Research Center of Zebrafish Models for Human Diseases and Drug Screening of Shandong Province. The zebrafish were maintained under a 14/10 h light/dark cycle at a temperature of 28 ± 0.5 °C in a closed flow-through system with charcoal-filtered tap water to ensure normal spawning. The healthy and sexually mature zebrafish are placed in the breeding tank, with a sex ratio of 1:1 and the zygotes are obtained the next day. After disinfection and washing of zygotes, they were transferred to zebrafish embryo culture water (5.0 mM NaCl, 0.17 mM KCl, 0.4 mM CaCl₂, 0.16 mM MgSO₄) for light-controlled culture at 28 °C for subsequent experiments.^{19,20}

Administration Treatment of Zebrafish. At 24 h postfertilization, the zebrafish embryos were removed from the egg membrane with 1 mg/mL Pronase E and were placed into 24-well plates (n = 10/well). The fish were randomly assigned to normal control, model (PTK787), positive control (PTK787 + Danhong injection or ferulic acid), and seven experimental groups (PTK787 + compounds). All treatments were performed twice and cultured in a light incubator (28 °C). 24 hours after administration, we can observe the number of the growth of blood vessels in zebrafish internode under a fluorescence microscope (AXIO, Zoom.V16).

Antimicrobial Activity Assay. The microbroth dilution method as demonstrated in earlier research^{21,22} was applied to evaluate the antimicrobial activity of tested compounds against methicillin-resistant *Staphylococcus aureus*, *B. thuringiensis*, *Staphylococcus epidermidis*, *E. piscicida*, *V. alginolyticus*, *P. syringae* pv. *actinidiae*, *Ralstonia solanacearum*, *Erwinia chrysanthemi*, *Pseudomonas plecoglossicida*, and *Escherichia coli*. CPL was used as a positive control.

TDDFT ECD Calculation. In general, conformational analyses were carried out via random searching in the Sybyl-X 2.0 using the MMFF94S force field with an energy cutoff of 5.0 kcal/mol.^{23,24} Subsequently, the conformers of compounds 1–4 were reoptimized using DFT at the b3lyp/6-311+g(d,p) level in MeOH by the Gaussian 09 program. The ECD spectra were simulated by the overlapping Gaussian function. To obtain the final spectra of 1–4, the simulated spectra of the conformers were averaged according to the Boltzmann distribution theory and their relative Gibbs free energy (ΔG).

■ ASSOCIATED CONTENT

SI Supporting Information

The Supporting Information is available free of charge at <https://pubs.acs.org/doi/10.1021/acsomega.4c02488>.

HRESIMS, IR, UV, and NMR spectra, data of ECD calculations of marchaeoglobins A–D (1–4), and strain identification information on *C. globosum* 162105 (PDF)

■ AUTHOR INFORMATION

Corresponding Authors

Weihua Jiao – State Key Laboratory of Cancer Gene and Related Gene, Research Center for Marine Drugs, Renji Hospital, School of Medicine, Shanghai Jiao Tong University, Shanghai 200127, China; orcid.org/0000-0003-4835-4775; Email: weihuajiao@hotmail.com

Shihai Xu – Department of Chemistry, College of Chemistry and Materials Science, Jinan University, Guangzhou 510632, China; Email: txush@jnu.edu.cn

Houwen Lin – State Key Laboratory of Cancer Gene and Related Gene, Research Center for Marine Drugs, Renji Hospital, School of Medicine, Shanghai Jiao Tong University, Shanghai 200127, China; orcid.org/0000-0002-7097-0876; Email: franklin67@126.com

Authors

Xianxian Miao – Department of Chemistry, College of Chemistry and Materials Science, Jinan University, Guangzhou 510632, China; State Key Laboratory of Cancer Gene and Related Gene, Research Center for Marine Drugs, Renji Hospital, School of Medicine, Shanghai Jiao Tong University, Shanghai 200127, China

Lili Hong – State Key Laboratory of Cancer Gene and Related Gene, Research Center for Marine Drugs, Renji Hospital, School of Medicine, Shanghai Jiao Tong University, Shanghai 200127, China

Zhiran Ju – Institute of Pharmaceutical Science and Technology, Collaborative Innovation Center of Yangtze River Delta Region Green Pharmaceuticals, Zhejiang University of Technology, Hangzhou 310014, China; orcid.org/0009-0000-1270-4468

Hongyan Liu – State Key Laboratory of Cancer Gene and Related Gene, Research Center for Marine Drugs, Renji Hospital, School of Medicine, Shanghai Jiao Tong University, Shanghai 200127, China

Ruyi Shang – State Key Laboratory of Cancer Gene and Related Gene, Research Center for Marine Drugs, Renji Hospital, School of Medicine, Shanghai Jiao Tong University, Shanghai 200127, China

Peihai Li – Engineering Research Center of Zebrafish Models for Human Diseases and Drug Screening of Shandong Province, Biology Institute, Qilu University of Technology (Shandong Academy of Sciences), Jinan 250103, China

Kechun Liu – Engineering Research Center of Zebrafish Models for Human Diseases and Drug Screening of Shandong Province, Biology Institute, Qilu University of Technology (Shandong Academy of Sciences), Jinan 250103, China; orcid.org/0000-0001-5461-5818

Bin Cheng – Institute of Marine Biomedicine, Shenzhen Polytechnic University, Shenzhen 518055, China

Complete contact information is available at: <https://pubs.acs.org/doi/10.1021/acsomega.4c02488>

Author Contributions

All listed authors contributed to this work. Weihua Jiao, Shihai Xu, and Houwen Lin: conceived and designed the experiments. Xianxian Miao: performed the chemical and antimicrobial assay experiments and wrote the manuscript. Hongyan Liu and Ruyi Shang: helped conducting the chemical experiments. Peihai Li and Kechun Liu: performed the proangiogenic activity assay experiments. Lili Hong, Zhiran Ju, and Bin Cheng: analyzed the data and revised the paper.

Notes

The authors declare no competing financial interest.

■ ACKNOWLEDGMENTS

This project is financially supported by the National Key Research and Development Program of China (no. 2022YFC2804100) and the National Natural Science Foundation of China (nos. 22137006 and 42376085). The authors acknowledge Engineer Yi-Zhen Yan and are grateful to his sacrifices in sponge sampling and guidance on NP systematic isolation.

■ REFERENCES

- (1) Wang, W.; Zeng, F. R.; Bie, Q.; Dai, C.; Chen, C. M.; Tong, Q. Y.; Liu, J. J.; Wang, J. P.; Zhou, Y.; Zhu, H. C.; Zhang, Y. H. Cytochalasins A-C: three merocytochalasins with a 2H-1,4-thiazine functionality from coculture of *Chaetomium globosum* and *Aspergillus flavipes*. *Org. Lett.* **2018**, *20*, 6817–6821.
- (2) Chen, C. M.; Zhu, H. C.; Li, X. N.; Yang, J. P.; Wang, J.; Li, G. T.; Li, Y.; Tong, Q. Y.; Yao, G. M.; Luo, Z. W.; Xue, Y. B.; Zhang, Y. H. Armochaeglobins A and B, two new indole-based alkaloids from the arthropod-derived fungus *Chaetomium globosum*. *Org. Lett.* **2015**, *17*, 644–647.
- (3) Hu, X. Y.; Li, X. M.; Yang, S. Q.; Li, X.; Wang, B. G.; Meng, L. H. Vercytochalasins A and B: Two unprecedented biosynthetically related cytochalasins from the deep-sea-sourced endozoic fungus *Curvularia verruculosa*. *Chin. Chem. Lett.* **2023**, *34*, 107516.
- (4) Zhu, H. C.; Chen, C. M.; Tong, Q. Y.; Zhou, Y.; Ye, Y.; Gu, L. H.; Zhang, Y. H. Progress in the Chemistry of Cytochalasins. In *Progress in the Chemistry of Organic Natural Products*; Kinghorn, A. D., Falk, H., Gibbons, S., Kobayashi, J., Asakawa, Y., Liu, J. K., Eds.; Springer International Publishing: Cham, 2021; pp 1–134.
- (5) Ding, X. M.; Ye, W. X.; Tan, B.; Song, Q. Y.; Chen, Y. C.; Liu, W.; Sun, L. L.; Tang, W.; Qiao, Y. L.; Zhang, Q. B.; Zhang, H.; Wang, Y.; Zhang, W.; Zhang, C.; et al. Talachalasin A-C, Undescribed Cytochalasins with a 16 β -Methyl or 2-Oxabicyclo [3.3.1] nonan-3-one unit from the Deep-Sea-Derived Fungus *Talaromyces muroii* sp. SCSIO 40439. *Chin. J. Chem.* **2023**, *41*, 915–923.
- (6) Qi, S.; Wang, Y.; Zheng, Z. H.; Xu, Q. Y.; Deng, X. M. Cytochalasins and sesquiterpenes from *Eutypella scoparia* 1–15. *Nat. Prod. Commun.* **2015**, *10*, 2027–2030.
- (7) Xin, X. Q.; Chen, Y.; Zhang, H.; Li, Y.; Yang, M. H.; Kong, L. Y. Cytotoxic seco-cytochalasins from an endophytic *Aspergillus* sp. harbored in *Pinellia ternata* tubers. *Fitoterapia* **2019**, *132*, 53–59.
- (8) Chen, C. M.; Wang, J. P.; Liu, J. J.; Zhu, H. C.; Sun, B.; Wang, J.; Zhang, J. W.; Luo, Z. W.; Yao, G. M.; Xue, Y. B.; Zhang, Y. H. Armochaetoglobins A-J: Cytochalasan alkaloids from *Chaetomium globosum* TW1–1, a fungus derived from the terrestrial arthropod *Armadiillidium vulgare*. *J. Nat. Prod.* **2015**, *78*, 1193–1201.
- (9) Ji, J. C.; Liu, C.; He, X. H.; Chen, G. L.; Qin, L. P.; Zheng, C. J. Salchaetoglobosins A and B: Cytochalasan alkaloids from *Chaetomium globosum* D38, a fungus derived from *Salvia miltiorrhiza*. *Fitoterapia* **2021**, *151*, 104874–104879.
- (10) Gao, W. X.; Sun, W. G.; Li, F. L.; Chai, C. W.; He, Y.; Wang, J. P.; Xue, Y. B.; Chen, C. M.; Zhu, H. C.; Hu, Z. X.; Zhang, Y. H. Armochaetoglobins A-I: cytochalasan alkaloids from fermentation

broth of *Chaetomium globosum* TW1-1 by feeding L-tyrosine. *Phytochemistry* **2018**, *156*, 106–115.

(11) Gao, W. X.; Jiang, R.; Zeng, H. X.; Cao, J.; Hu, Z. X.; Zhang, Y. H. Armochaetoglasins L and M, new cytochalasans from an arthropod-derived fungus *Chaetomium globosum*. *Nat. Prod. Res.* **2022**, *38*, 1599–1605.

(12) Ruan, B. H.; Yu, Z. F.; Yang, X. Q.; Yang, Y. B.; Hu, M.; Zhang, Z. X.; Zhou, Q. Y.; Zhou, H.; Ding, Z. T. New bioactive compounds from aquatic endophyte *Chaetomium globosum*. *Nat. Prod. Res.* **2018**, *32*, 1050–1055.

(13) Qi, J.; Jiang, L.; Zhao, P. P.; Chen, H. Y.; Jia, X. P.; Zhao, L. Y.; Dai, H.; Hu, J. S.; Liu, C. H.; Shim, S. H.; Xia, X. K.; Zhang, L. X. Chaetoglobosins and azaphilones from *Chaetomium globosum* associated with *Apostichopus japonicus*. *Appl. Microbiol. Biotechnol.* **2020**, *104*, 1545–1553.

(14) Ishiuchi, K. I.; Nakazawa, T.; Yagishita, F.; Mino, T.; Noguchi, H.; Hotta, K.; Watanabe, K. Combinatorial generation of complexity by redox enzymes in the chaetoglobosin A biosynthesis. *J. Am. Chem. Soc.* **2013**, *135*, 7371–7377.

(15) Cui, C. M.; Li, X. M.; Li, C. S.; Proksch, P.; Wang, B. G. Cytoglobosins A-G, cytochalasans from a marine-derived endophytic fungus, *Chaetomium globosum* QEN-14. *J. Nat. Prod.* **2010**, *73*, 729–733.

(16) Ichihara, A.; Katayama, K.; Teshima, H.; Oikawa, H.; Sakamura, S. Chaetoglobosin O and other phytotoxic metabolites from *Cylindrocladium floridanum*, a causal fungus of alfalfa black rot disease. *Biosci. Biotechnol. Biochem.* **1996**, *60*, 360–361.

(17) Oikawa, H.; Murakami, Y.; Ichihara, A. Useful approach to find the plausible biosynthetic precursors of secondary metabolites using P-450 inhibitors: postulated intermediates of chaetoglobosin A. *J. Chem. Soc., Perkin Trans. 1* **1992**, 2949–2953.

(18) Sekita, S.; Yoshihira, K.; Natori, S. Chaetoglobosins, cytotoxic 10-(indol-3-yl)-[13] cytochalasans from *Chaetomium* spp. IV. ¹³C-nuclear magnetic resonance spectra and their application to a biosynthetic study. *Chem. Pharm. Bull.* **1983**, *31*, 490–498.

(19) Jin, T. Y.; Li, P. L.; Wang, C. L.; Tang, X. L.; Cheng, M. M.; Zong, Y.; Luo, L. Z.; Ou, H. L.; Liu, K. C.; Li, G. Q. Racemic bisindole alkaloids: structure, bioactivity, and computational study. *Chin. J. Chem.* **2021**, *39*, 2588–2598.

(20) Yan, L. H.; Li, P. H.; Li, X. M.; Yang, S. Q.; Liu, K. C.; Wang, B. G.; Li, X. Chevalinulins A and B, proangiogenic alkaloids with a spiro [bicyclo [2.2.2] octane-diketopiperazine] skeleton from deep-sea cold-seep-derived fungus *Aspergillus chevalieri* CS-122. *Org. Lett.* **2022**, *24*, 2684–2688.

(21) Song, T. F.; Chen, M. X.; Ge, Z. W.; Chai, W. Y.; Li, X. C.; Zhang, Z. Z.; Lian, X. Y. Bioactive penicypyrrodiether A, an adduct of GKK1032 analogue and phenol A derivative, from a marine-sourced fungus *Penicillium* sp. ZZ380. *J. Org. Chem.* **2018**, *83*, 13395–13401.

(22) Sun, C.; Ha, Y.; Liu, X.; Wang, N.; Lian, X. Y.; Zhang, Z. Isolation and Structure Elucidation of New Metabolites from the Mariana-Trench-Associated Fungus *Aspergillus* sp. SY2601. *Molecules* **2024**, *29*, 459.

(23) Gui, Y. H.; Jiao, W. H.; Zhou, M.; Zhang, Y.; Zeng, D. Q.; Zhu, H. R.; Liu, K. C.; Sun, F.; Chen, H. F.; Lin, H. W. Septosones A-C, in vivo anti-inflammatory meroterpenoids with rearranged carbon skeletons from the marine sponge *Dysidea septosa*. *Org. Lett.* **2019**, *21*, 767–770.

(24) Wang, J.; Mu, F. R.; Jiao, W. H.; Huang, J.; Hong, L. L.; Yang, F.; Xu, Y.; Wang, S. P.; Sun, F.; Lin, H. W. Meroterpenoids with Protein Tyrosine Phosphatase 1B Inhibitory Activity from a *Hyrtios* sp. Marine Sponge. *J. Nat. Prod.* **2017**, *80*, 2509–2514.